Research Square

Preprints are preliminary reports that have not undergone peer review.
They should not be considered conclusive, used to inform clinical practice,
or referenced by the media as validated information.

Synthesis and Biological Evaluation of Novel Uracil Derivatives as Thymidylate Synthase Inhibitors

Manzoor Ahmad Mir (drmanzoor@kashmiruniversity.ac.in)
University of Kashmir https://orcid.org/0000-0003-3297-1402

Research Article

Keywords: Breast cancer, drug discovery, thymidylate synthase, uracil derivatives, one-pot synthesis, Cell cycle

Posted Date: September 14th, 2022

DOI: https://doi.org/10.21203/rs.3.rs-2053542/v1

License: This work is licensed under a Creative Commons Attribution 4.0 International License.
Read Full License

Abstract

Aim

To synthesize novel uracil derivatives targeting thymidylate synthase for the treatment of high-grade malignancies such as breast cancer.

Background

Cell division is driven by nucleic acid metabolism, and thymidylate synthase (TYMS) catalyses a rate-limiting step in nucleotide synthesis. As a result, TYMS has emerged as a critical target in chemotherapy. 5-fluorouracil (5-FU) is currently being used to treat a wide range of cancers, including breast, pancreatic, head and neck, colorectal, ovarian, and gastric cancers.

Objectives

The objective of this study was to establish a new methodology for the low-cost, one-pot synthesis of uracil derivatives (UD-1 to UD-5) and to evaluate their therapeutic potential in BC cells.

Methods

One-pot organic synthesis processes using a single solvent were used for the synthesis of drug analogues of Uracil. Integrated bioinformatics using GEPIA2, UALCAN and KM plotter were utilized to study the expression pattern and prognostic significance of TYMS, the key target gene of 5-fluorouracil in breast cancer patients. Cell viability, cell proliferation, and colony formation assays were used as in-vitro methods to validate the in-silico lead obtained.

Results

BC patients showed high levels of TYMS, and high expression of TYMS was found associated with poor prognosis. In silico studies indicated that synthesized uracil derivatives have a high affinity for TYMS. Notably, the uracil derivatives dramatically inhibited the proliferation and colonization potential of BC cells in vitro.

Conclusion

In conclusion, our study identified novel uracil derivatives as promising therapeutic options for breast cancer patients expressing the augmented levels of TYMS.

1. Introduction

Due to the long-standing anticancer potency of 5-Fluorouracil, uracil have been a top priority for many researchers, notably in the field of drug discovery and synthetic accessibility (23, 31). Uracil derivatives exhibit bactericidal, herbicidal, and insecticidal activity, with antiviral and anticancer activity being particularly notable (33, 14). Their antiviral activity is based on inhibiting a critical stage in the viral replication pathway, which results in robust effectiveness against HIV, hepatitis B and C, and herpes viruses, among others (40, 32). 5-Fluorouracil and 5-Chlorouracil were the first uracil derivatives to exhibit pharmacological activity and approved for use in the treatment of several ailments (43, 3). Recently, scientists have focused increasing attention on uracil derivatives; several of the most clinically significant compounds are illustrated in **Figure. S1 (Supplementary Information)** (29). Numerous changes to uracil have been made to address toxicity concerns in the synthesis of derivatives with improved pharmacological and pharmacokinetic features (increased bioactivity, selectivity, metabolic stability, absorption, and decreased toxicity) (29, 23, 14). The development of novel uracil derivatives and fused uracil derivatives as bioactive agents is dependent on substituent changes at various places on the pyrimidine ring.

One-pot organic synthesis processes using a single solvent have sparked considerable attention among researchers due to their low cost, environmental friendliness, the potential for high yield products, and insights into green chemistry (8). Green chemistry techniques are crucial because they minimize waste, byproducts, energy use, and expense (8). The capacity to execute multistep reactions in a single pot could significantly increase their efficiency, both economically and environmentally. Due to its immense range of applications in synthetic chemistry, the synthesis of novel heterocyclic molecules has always been a subject of significant interest. Because heterocyclic compounds are abundant in nature and are required for life to exist. Among them, heterocyclic compounds containing the uracil moiety are of interest because they exhibit a variety of pharmacological and biological properties. Uracil and its derivatives are critical starting materials for the synthesis of a wide variety of chemical compounds, pharmaceutical drugs, and intermediates (7, 15, 16). For example, Tegafur-uracil, a pyrimidine derivative is a chemotherapeutic agent used in cancer treatment, most commonly colon cancer (1). Thus, developing novel uracil derivatives is a critical and essential endeavor in organic chemistry. In addition to the aspects discussed in the literature, attempts were made to establish a new methodology for the low-cost, one-pot synthesis of uracil derivatives.

Globally, breast cancer (BC) is currently the most prevalent malignancy among women and the second leading cause of cancer-related death (36, 35, 21). Current treatment methods include breast ectomy, radiation therapy (RT), chemotherapy therapy (CT), hormone therapy (HT), and immunological therapy (11, 42, 25, 22, 17). Treatments are decided by each patient's clinicopathologic and tumor grade features (25, 28). Despite advances in diagnostics and therapy, BC mortalities are highest owing to metastatic tumors, tumor relapse, and the development of chemoresistance resulting in poor prognosis (20). Thus, there is an urgent need to develop and explore novel therapeutic regimens for BC patients, particularly for triple-negative breast cancer (TNBC) patients, as chemotherapy is the mainstay of therapeutic protocol

for these patients (18, 19). Due to the high proliferative nature of tumor cells, raw material for the synthesis of macromolecules viz proteins and DNA and vastly required (34). The rate-limiting step in DNA synthesis is catalyzed by thymidylate synthase (TS), which is the only de novo cellular source of dTTP (9). As a result, TYMS has emerged as a critical target in cancer chemotherapy, especially breast cancer (30). 5-fluorouracil (5-FU) targeting TYMS is presently used in the treatment of several malignancies including breast, pancreatic, head, and neck, colorectal, ovarian, and gastric cancers (37, 44, 26). Despite a favorable initial response to 5-FU, BC patients frequently develop chemoresistance due to the inherent nature of tumor cells to mutate, highlighting an urgent need to investigate new therapeutic options targeting TYMS (45, 24). In the present study, we synthesized novel uracil derivatives and evaluated their anticancer activity using *in silico* and *in vitro* approaches. We further explored the expression pattern and prognostic significance of TYMS in BC patients, key target gene of 5-fluorouracil. *In silico* analysis showed high affinity of uracil derivatives in contrast to 5-FU. Additionally, *in vitro* studies demonstrated that synthesized derivatives exhibited substantial cytotoxic activity and the potential to impede colonization of breast tumor cells. Taken together, the findings suggest that new uracil analogues may be promising therapeutics for breast cancer in combination with current treatment regimens.

2. Results And Discussion

2..1 Chemistry

One-Pot Synthesis of Uracil derivatives (UD-1 to UD-5)

Initially, charged 6-chlorouracil (7.75 g, 0.05 M) and potassium carbonate (9.14 g, 0.06 M) were mixed in 50 mL DMF in 250 mL RBF, followed by halogenated of 1-(bromomethyl) benzene (10 g, 0.05 M), the reaction mixture was stirred for 8 h at RT. Then, with further addition of potassium carbonate (7.31 g, 0.0529 M) and methyl iodide (15.02 g, 0.10 M) the reaction mixture was further stirred overnight at room temperature. After that, the charged piperazine (4.52 g, 0.05 M) or piperidine or 3-aminopiperidine (9.10 g, 0.05 M) was added to the reaction mixture and heated at 80 ˚C for 8 h to get compounds 3, UD-4, and 5 respectively. Finally, the reaction mixture of compound 3 was separately treated with acetone, water, and potassium carbonate with different chloroformates to give UD-1, UD-2, and UD-3. In another reaction, the Moc-L-Valine (9.22g, 0.05 M) was added to the reaction mixture (5) in presence of coupling reagent HATU (40.23 g, 0.10 M) and triethylamine (10.71 g, 0.10M) and stirred the mixture at RT for 25 min. After the completion of the reaction, water was added and the product was extracted in ethyl acetate, the organic layer was dried over sodium sulfate, and the solvent was removed under reduced pressure. The desired product was purified by column chromatography to get the title compound (**UD-5**). The steps for the synthesis of the uracil derivatives are displayed in Fig. 1 and the chemical structures of the final products are given in Fig. 2.

Heptyl-4-(3-(4-fluorobenzyl)-1-methyl-2,6-dioxohexahydropyrimidin-4-yl)piperazine-1-carboxylate (UD-1)

Yield: 55%, mp; 194–195˚C; White solid powder;^{1}H-NMR: δ = 0.85–0.88 (t, 3 H, -CH_3), 1.27–1.31 (broad, 8 H, -CH_2), 1.55–1.63 (m, 2 H, -CH_2), 2.80 (broad, 4H, -CH_2), 3.32 (s, 3 H, -N-CH_3), 3.49–3.63 (broad, 3 H, -CH_2), 4.05–4.08 (t, 2 H, -O-CH_2), 5.16 (s, 2 H, Ar-CH_2-), 5.33 (s, 1 H, -CH), 7.02–7.07 (t, 1 H, ArH) 7.09–7.13(m, 2 H, ArH), 7.23–7.28 (m, 1 H, ArH) ppm. Mass: ($C_{24}H_{33}FN_4O_4$) *m/z = 460.25, M + H = 461.1.*

Octyl-4-(3-(4-fluorobenzyl)-1-methyl-2,6-dioxohexahydropyrimidin-4-yl)piperazine-1-carboxylate (UD2)

Yield: 57%, mp; 180–191˚C; White solid powder; ^{1}H-NMR: δ = 0.85–0.88 (t, 3 H, -CH_3), 1.02–1.40 (m, 12 H, -CH_2), 1.59–1.80 (t, 3 H, -CH_2), 2.82 (broad, 4H, -CH_2), 3.31 (s, 3 H, -N-CH_3), 3.42–3.52(broad, 4 H, -CH_2), 4.05–4.09 (t, 2 H, -O-CH_2), 5.08 (s, 2 H, Ar-CH_2-), 5.34 (s, 1 H, -CH), 6.89–6.94 (q, 1 H, ArH) 6.96–6.98 (d, 2 H, ArH), 7.26–7.31(q, 1 H, ArH) ppm. Mass: ($C_{25}H_{35}FN_4O_4$) *m/z = 474.26, M + H = 475.1.*

Heptyl-4-(1-methyl-3-(4-nitrobenzyl)-2,6-dioxohexahydropyrimidin-4-yl)piperazine-1 carboxylate (UD-3)

Yield: 59%, mp; 197–198˚C; White solid powder; 1H-NMR: δ = 0.86–0.88 (t, 3 H, -CH3), 1.21–1.24 (broad, 10 H, -CH_2), 1.45–1.57 (m, 3 H, -CH_2), 2.80 (broad, 4H, -CH_2), 3.23 (s, 3 H, -N-CH_3), 3.47–3.56 (broad, 4 H, -CH_2), 3.99–4.03 (t, 2 H, -O-CH_2), 5.13 (s, 2 H, Ar-CH_2), 5.33 (s, 1 H, -CH), 7.25–7.34 (d, 2 H, ArH) 8.11–8.13(d, 2 H, ArH) ppm. Mass: ($C_{24}H_{33}N_5O_6$) m/z = 487.24, *M + H = 488.*

1-(4-Fluorobenzyl)-3-methyl-6-(piperidin-1-yl)dihydropyrimidine-2,4(1H,3H)-dione (UD-4)

Yield: 57%, mp; 175–176˚C; White solid powder;^{1}H-NMR: δ = 1.63 (m, 6 H,-CH_2), 2.86 (s; 4 H, -CH_2), 5.02 (s, 2 H, -CH2), 5.32 (s, 1 H, -CH), 6.98 (t, 2 H, Ar-H), 7.22 (m, 3 H, Ar-H) ppm. ^{13}C NMR δ = 23.77, (-CH2), 25.33 (-CH2), 27.84 (-CH3), 47.22 (-CH2), 52.44 (-CH2), 89.78 (-CH), 115 (Ar-C), 128.95 (Ar-C), 132.17 (Ar-C), 152 (-N-CO-N-), 160.37 (-C-), 163.36 (-N-CO-C-) ppm. *Mass ($C_{17}H_{22}FN_3O_2$) m/z = 319.17*

Methyl-1-1-(3-(2-cyanobenzyl)-1-methyl-2,6-dioxo-1,2,3,6-tetrahydropyrimidin-4-yl)piperidin-3-ylamino)-3-methyl-1-oxobutan-2-ylcarbamate (UD-5)

Yield: 57%, mp; 184–185˚C; White solid powder;^{1}H-NMR: δ = 0.71 (dd, 6 H,-CH_3), 1.29 (m; 2 H, -CH_2), 1.74–1.79 (m, 3 H, -CH_2), 2.3 (m, 1 H, -CH_2), 2.46 (s, 3 H, CH_2), 2.59 (m, 1 H, -CH_2), 2.8 (d, 1 H, -CH_2), 3.08 (s, 3 H, -N-CH_3), 3.48 (s, 3 H, -O-CH_3), 3.71 (t, 2 H, -CH_2), 4.92 (q, 2 H, -CH_2), 5.25 (s, 1 H, -CH), 6.97 (m, 3 H, Ar-H), 7.09 (d, 1 H, Ar-H), 7.29 (d, 1 H, Ar-H), 7.95 (d, 1 H, -NH). *Mass ($C_{25}H_{32}N_6O_5$) m/z = 496.56, M + H = 497.2481.*

It is highly noted that in the available literature, generally in benzylation and methylation reactions base like sodium hydride in dimethylformamide have been used which is highly dangerous in the context of safety, environment pollutant and it also results in poor yield, impure compounds. In our simple protocol, we used low-cost, ecofriendly, and safe inorganic base potassium carbonate in dimethylformamide solvent in one pot during four steps which is one of the major advantages of our protocol. In addition, we got higher percentage yields of products. Initially, we have synthesized N-substituted uracil analogs in

high yields by simple N-benzylation of 6-chlorouracil with different halogenated benzyl halides and N-methylation by methyl iodide respectively, under catalyst-free conditions in DMF solvent. Then the chlorine atoms of N-substituted uracil derivatives were substituted with piperazine, piperidine, and 3-aminopiperidine, respectively. In the final step, the N-substitution of the piperazine ring was carried out by treating it with different alkyl containing chloroformates in the same pot under similar conditions for the formation of compounds **UD-1-UD-4**. Simultaneously, under similar conditions in the same solvent amino acid coupling reaction was done in presence of coupling reagent HATU (1-bis(dimethylamino)methylene-1H-1,2,3-triazolo[4,5-b]pyridinium-3-oxid hexafluorophosphate) for the formation of target compounds **UD-5**. The whole synthesis has been done in one solvent in one pot that results in the reduction of industrial waste, affluent generation, and overall good yields (55–59%) of final products.

A reasonable mechanism for the formation of uracil derivatives is shown in Fig. 3. The reaction conditions were optimized using various solvents, bases. The yields ranged from 55 to 59%. A perusal of these indicates that the DMF and inorganic base was the best one; resulting in higher yield and best conversion. During the optimization of organic and inorganic bases were used. It was observed that during organic bases, the reaction was completed at a faster rate, but less conversion was observed. The percentage of yield was increased while using inorganic bases under DMF solvent. Hence, throughout the reaction, potassium carbonate as base and DMF as solvent were used. The proposed structures of uracil derivatives (**UD-1 to UD-5)** were well supported by analytical and spectroscopic data. All the derivatives were found as solids, stable to air, had good yields, and quite soluble in ethyl acetate, methanol, ethanol, chloroform, DMSO, DMF. The characteristic signal from the CH_3N- group in the ^1H NMR spectrum was observed as a singlet at ~ 2.90–3.10 ppm, methine proton of uracil ring CH- was observed at 5.00 -5.35 ppm, benzylic proton -CH at 4.86–5.37 ppm, aromatic protons Ar-H appeared in the range of 7.00–8.10 ppm, piperazine protons resonates at 1.50–3.80 ppm, methyl protons appeared in the range of 2.90–3.40 ppm, and methoxy protons -OCH_3 appeared in the range of 3.40–3.75 ppm. The ^1H NMR spectra of uracil derivatives (**UD-1 to UD-5**) are shown in **Figure S2-S6 (Supplementary Information**). Elemental analyses and ESI-MS spectra illustrated the compositions of synthesized compounds. The mass spectra of **UD-1 to UD-5** showed the peaks at m/z values of 460.25, 474.26, 487.24, 319.17 and 496.56 corresponding to **UD-1**, **UD-2, UD-3, UD-4** and **UD-5**.

Drug-likeness

Oral bioavailability (a measure of drug-likeness) is one of the major parameters for developing bioactive molecules as effective pharmaceutical agents. Parameters like good intestinal absorption, reduced molecular flexibility, low polar surface area, or total hydrogen bond count, are essential factors for the prediction of good oral bioavailability (41). Drug properties like membrane permeability and bioavailability are associated with some basic molecular descriptors: molecular mass, hydrogen bond acceptor and donor count, and log P (partition coefficient) in a molecule (12). These properties were originally used by Lipinski (12) to formulate his well-known “Rule of five”. The rule stands, most molecules with good membrane permeability have molecular mass < 500 Da, number of hydrogen bond acceptors < 10, number of hydrogen bond donors < 5, and log P < 5. This rule is commonly used to

evaluate the suitability of a drug for oral administration. This rule is widely used as a filter for the screening of molecules with drug-like properties. Generally, a compound that fulfills at least three points out of five is said to follow Lipinski's rule. A poor permeation or absorption is more likely to occur when there are more than 5 H-bond donors and 10 H-bond acceptors. Therefore, all these molecular properties of the mentioned uracil derivatives were calculated using MarvinSketch and are displayed in Table 1, showing all uracil derivatives have molecular masses lower than 500, contain hydrogen bond acceptors < 10 and number of hydrogen bond donors < 5. Moreover, the uracil derivatives have lower log P, molar refractivity, and polar surface areas than the values recommended by Lipinski's rule. Thus, the synthesized uracil derivatives fully meet all the five criteria of Lipinski's rule, hence having good oral bioavailability.

Table 1
Molecular properties of uracil derivatives show their oral bioavailability and drug-likeness.

Derivative	Molecular mass/u	Log P	Hydrogen bond acceptors	Hydrogen bond donors	Molar refractivity/ (m^3 M^{-1})	Polar surface area/ °A2
UD1	462.56	-3.80	4	0	122.75	73.40
UD2	476.5	-4.24	4	0	127.35	73.40
UD3	487.4	-4.04	6	0	133.45	116.54
UD4	319.38	-2.30	3	0	85.27	43.86
UD5	498.5	-1.62	6	2	131.15	135.08

2.2 Molecular Docking Studies

Uracil derivatives show a high docking affinity for thymidylate synthase

CB-Dock by default predicts five binding cavities and based on experimental information of the binding site of the co-crystallized substrate of thymidylate synthase, we proved that the correct binding site is among the predicted cavities (Fig. 4A). Pyrimidine analog namely 5-Fluorouracil (5-FU) has been approved by FDA for a variety of cancers including gastric adenocarcinoma and breast cancer (13). Metabolite of 5-FU by name fluorodeoxyuridine monophosphate (FdUMP) competes with normal substrate dUMP and thus prevents its binding with thymidylate synthase (13). As it is clear that FdUMP but not 5-FU binds with thymidylate synthase thus we used the former rather than the latter as a positive control in the docking study and compared the binding affinity of six novel molecules with FdUMP. All the newly tested molecules showed higher binding affinity than FdUMP (− 6.7 kcal/mol). However, two molecules namely UD4 and UD5 exhibited the highest inclination towards the predefined site of thymidylate synthase. While UD- showed a binding affinity value of − 8.3 kcal/mol, UD4 showed a binding affinity of − 8.0 kcal/mol **(**Fig. 4B**).** The ligand-receptor interaction is more favorable when the binding

affinity values are more negative. Thus, the binding affinity value is more negative for UD5 and UD4 suggests its more inclination towards thymidylate synthase compared to FdUMP.

The interaction profile of the five UDs in the docked state with thymidylate synthase was generated. Expectedly, the two most potent molecules showed relatively more interactions than the third strong binder against thymidylate synthase. UD4 formed four hydrophobic interactions (ILE 108, TRP 109, LEU 192, PHE 225) and two hydrogen bonds with amino acid residues GLN 214 and ASP 218 of binding groove. UD5 which was predicted by flexible docking as the most powerful molecule against the binding groove of thymidylate synthase also showed an extensive interaction profile. It displayed three hydrophobic interactions, two with LEU 192 and one with ASP 218. Furthermore, three hydrogen bonds were seen between ligand 5 and three residues (ARG 50, ASP 218, and TYR 258) of thymidylate synthase (Fig. 4A). Our results align well with the study where enhanced ligand efficiency has been attributed to hydrophobic interactions (8). All the novel molecules and the known binder FdUMP bind at the experimentally certified binding site of dUMP, the substrate of thymidylate synthase, which further authenticates the reliability of our findings **Figure S7** (**Supplementary Information**).

2.3. Expression pattern & prognostic significance of TYMS in BC patients

TYMS is upregulated in BC Patients.

Using the TCGA BrCa dataset of the Gepia2 online portal, the expression of TYMS was analyzed, and it was revealed that TYMS is highly overexpressed in breast cancer patients in contrast to normal women. TYMS was found to be upregulated with a $\log_2$ FC of 2.223, (p-value of 1.58e-179) Fig. 5A. Also, we analyzed the TYMS expression within BC subclasses and women with different ethnicities using the UALCAN portal and it was found that among different subclasses of BC, TYMS was highly upregulated in TNBC and women with African-American ethnicity Fig. 5B, C, **and D**.

High expression of TYMS affects the prognosis of BC patients.

The prognostic significance of the TYMS expression was analyzed using the online open database, the Kaplan-Meier Plotter. The KM plots demonstrated that BC patients with high expression of TYMS had worse relapse-free survival and overall survival ($p < 0.05$) Fig. 5E, F. Also, BC patients with reduced levels of TYMS had better relapse-free survival and overall survival. These results indicate that targeting TYMS may prolong the survival of breast cancer patients, in particular the TNBC patients who solely rely on chemotherapeutic regimens.

2.4. In vitro anti-cancer activity

Uracil derivatives possess potent anti-proliferative activity

To examine whether UDs, possessed anti-cancer activity, we performed a preliminary assay of cell viability on MDA-MB-231 cells. UD-1, UD-2, UD-3, UD-4 and UD-5 were given at 50 µM conc. and cells were

incubated with drugs for 72 h. MTT assay analysis revealed that UD-1, UD-2, and UD-4 possessed high anti-cancer activity compared to UD-3, and UD-5 Fig. 6A. The three derivatives UD-1, UD-2, and UD-4 were selected for further analysis in a panel of breast cancer cell lines.

To investigate the effect of UD-1, UD-2, and UD-4, BC cell lines were treated with different concentrations of the selected UDs. The effects of UDs on the survival of BC cells were assessed by MTT assay. As shown in Fig. 6B, C, D **&** Fig. 7, UDs inhibited cell proliferation in a time- and concentration-dependent manner. UD1 exhibited a log IC50 value of 1.86 μM, 1.89 μM, 2.0 μM, and 1.89 μM in MDA-MB-231, MDA-MB-468, MCF-7, and 4T1 cells respectively. UD2 exhibited a log IC50 value of 1.51 μM, 1.85 μM, 1.86 μM, and 1.83 μM in MDA-MB-231, MDA-MB-468, MCF-7, and 4T1 cells respectively. UD4 exhibited a log IC50 value of 1.3 μM, 1.7 μM, 1.8 μM, and 1.6 μM in MDA-MB-231, MDA-MB-468, MCF-7, and 4T1 cells respectively **Table S8** (**Supplementary Information**).

Among the three potent UDs, UD-4 demonstrated high anti-proliferative activity *in vitro*, with the lowest IC50 compared to UD-1 & UD-2. Among different BC cell lines, the TNBC cell lines showed more sensitivity towards UDs and had lower IC_{50} compared to ER + cell line MCF-7.

Effect of Uracil derivatives on colony formation potential of MDA-MB-231 cells

To further validate the anti-cancer activity of UDs, a colony formation assay was performed in BC cell line MDA-MB-231 Fig. 8. Treatment with UDs showed dose-dependent inhibition of colony formation potential of breast tumor cells. Among the UDs, UD-4 showed the highest reduction in colony formation potential of tumor cells. UD-1 and UD-2 had less effect on colony formation in MDA-MB-231 cells, however, the small size of colonies in the treated wells of UD1 and UD2 demonstrates that UD1 and UD2 restrict the growth of tumor cells. These results demonstrate that UDs can limit the growth of breast tumor metastases and may be a promising approach in reducing the colonization of tumor cells at metastatic niches.

3. Conclusion

In summary, we presented a new efficient, low-cost, eco-friendly highly scalable, and one-pot method for the synthesis of five uracil derivatives from readily available 6-chlorouracil and their biological activity in TNBC. The key steps of our synthetic efforts rely on 1) N-benzylation, 2) N-methylation, 3) substitution and 4) amino acid coupling. The target compounds were obtained in overall good yields (**55–57%**). Spectroscopic and analytical techniques fully characterized the target compounds. 5-FU is an FDA-approved drug for the treatment of several malignancies including BC. Our study identified **UD4**, the most potent derivative with micromolar potency against TYMS. Also, **UD4** showed a good drug-like profile (e.g., aqueous solubility and ligand efficiency metric), along with an *in vitro* pharmacokinetic profile. Further exploration of the potency of **UD4** in mouse mammary TNBC models is required. Overall, the study identified novel uracil derivatives as potent drug candidates for BC patients with high expression of TYMS which indicates their quite bright future in the field of drug discovery.

4. Materials And Methods

All the reagents and chemicals used are of analytical and molecular biology grade and were obtained from the highest grade available from Sigma Aldrich, Acros organics, Spectrochem, Loba Chem, Survival Technology, and Rankem Laboratories, and were used without purification. TLC was performed on Merck TLC Silica gel 60 F254 plates eluting with specific solvents and samples were made visual with a UV lamp, Silica gel (60–120 mesh) was used for column chromatography. Melting points were measured on an Electrothermal 9100 apparatus. High-resolution mass spectra were measured were Bruker. The measurement was run in positive ion mode. ^{1}H NMR was obtained using Bruker (400 MHz) spectrometer in DMSO and $CDCl_3$ with tetramethylsilane as an internal standard. All NMR spectra at room temperature (RT) were determined in DMSO-d_6 and $CDCl_3$. Chemical shifts are reported in parts per million (δ) downfield from an internal tetramethylsilane reference. Coupling constants (J values) are reported in hertz (Hz), and spin multiplicities are indicated by the following symbols: s (singlet), d (doublet), t (triplet), q (quartet), m (multiplet). *Signals related to DMSO and residual ethanol, are indicated on the spectra.

4.1 Chemistry

4.1.1. *Synthesis of 6-Chloro-1-(4-fluorobenzyl)dihydropyrimidine-2,4(1H,3H)-dione* (1)

Charged 6-Chlorouracil (10 g, 0.06824 moles) and diisopropylethylamine (18.52 g, 0.1432 moles) followed by addition of 50 ml DMF this mixture was stirred 10 min. at RT then 1-(bromomethyl)-4-fluorobenzene (12.90 g, 0.06824 moles) was added to it, this reaction mass stirred 8 h at room temperature, after completion of reaction 150 ml water was added into it, the title product was isolated by filtration. Weight: 15.65g (90%).

4.1.2. *Synthesis of 6-Chloro-1-(4-fluorobenzyl)-3-methyldihydropyrimidine-2,4(1H,3H)-dione* (2)

Charged 6-Chloro-1-(4-fluorobenzyl) dihydropyrimidine-2,4(1H,3H)-dione (10 g, 0.0327 moles) in 100 ml acetone followed by potassium carbonate (13.57 g, 0.0981 moles) this reaction mass stirred 15 min. at RT followed by the addition of methyl iodide (11.14 g, 0.0784 moles), this reaction mass was stirred overnight, after the reaction was judged to be completed water was added to it and the product was isolated by filtration, and the product was dried to give the title compound. Weight: 9.60 g (91.0%)

4.1.3. *Synthesis of 1-(4-fluorobenzyl)-3-methyl-6-(piperazin-1-yl) dihydropyrimidine-2,4(1H,3H)-dione* (3)

Charged 6-Chloro-1-(4-fluorobenzyl)-3-methyldihydropyrimidine-2,4(1H,3H)-dione (9.0 g, 0.0334 moles) followed by 45 ml DMF and potassium carbonate (9.25 g, 0.0669 moles) was added then piperazine (3.60 g, 0.0417 moles) then the reaction mass was heated to 80°C, then the reaction mass stirred until

completion of reaction then cooled to RT water was added into it then MDC was added, the organic layer was separated, the organic layer dried with sodium sulfate solvents was removed under reduced pressure to give the title compound. Weight: 9.50 g (89.0%).

4.1.4. *Synthesis of Uracil Derivatives (UD-1 to UD-3)*

To the solution of 1-(4-fluorobenzyl)-3-methyl-6-(piperazin-1-yl)dihydropyrimidine-2,4(1H,3H)-dione (10.0 g, 0.0314 moles) in 100 ml acetone and 5 ml water, (8.68 g, 0.0628 moles) of potassium carbonate was added and the reaction mass was stirred for 10 min. at room temperature followed by the addition of 1.20 mole equivalents of chloroformates separately. After that, the reaction mixture was again stirred for 2 h at RT followed by the addition of water, product was extracted with ethyl acetate, purified by column chromatography to afford the UD-1 & UD-2. For the preparation of UD-3, 1-(4-nitrobenzyl)-3-methyl-6-(piperazin-1-yl) dihydropyrimidine-2,4(1H,3H)-dione was used instead of 1-(4-fluorobenzyl)-3-methyl-6-(piperazin-1-yl)dihydropyrimidine-2,4(1H,3H)-dione.

4.1.5. *Synthesis of Uracil Derivative (UD-4)*

Charged 6-Chloro-1-(4-fluorobenzyl)-3-methyldihydropyrimidine-2,4(1H,3H)-dione (9.0 g, 0.0334 moles) followed by 45 ml DMF and potassium carbonate (9.25 g, 0.0669 moles) was added then piperidine (3.60 g, 0.0417 moles) then the reaction mass was heated to 70–80°C, then the reaction mass stirred until completion of reaction then cooled to RT water was added into it then MDC was added, the organic layer was separated, the organic layer dried with sodium sulfate solvents was removed under reduced pressure to gives the title compound. Weight: 7.50 g (79.0%).

4.1.6. Synthesis of 2-((6-(3-aminopiperidin-1-yl)-3-methyl-2,4-dioxotetrahydropyrimidin-1(2H)-yl)methyl)benzonitrile (5)

Charged **2** (9.0 g, 0.03 M) was dissolved in 45 mL DMF followed by the addition of potassium carbonate (9.25 g, 0.06 M). Then piperidin-3-amine (6.83 g, 0.039 M) was added, and the reaction mixture was heated at 80°C, until the completion of the reaction. Then the reaction mixture was cooled to RT and water was added to it and extracted with dichloromethane. The organic layer was separated and was dried over sodium sulfate. Finally, the solvent was removed under reduced pressure for the formation of compound **5** (9.81 g, 87%).

4.1.7. *Synthesis of Uracil Derivative (UD-5)*

Charged **5** (9.0 g, 0.028 M) was initially dissolved in 90 mL dichloromethane, then HATU (16.12 g, 0.042 moles) was added to the solution followed by Moc-L-Valine (5.20 g, 0.029 moles) then TEA (5.72 g, 0.056 moles), the resulting solution was stirred RT till completion of the reaction. Finally, 20 mL of water was added into it an organic layer was separated and dried over sodium sulfate and the left solvent was removed under reduced pressure to give derivative UD-5.

4.2. Molecular docking and Integrated Bioinformatic Analysis

4.2.1 *In silico evaluation of Uracil derivatives with Thymidylate Synthase (TYMS)*

Human thymidylate synthase crystal structure was fetched from Protein Data Bank (PDB ID: 5X66) (2). Chimera software (version 1.11.2) was used to expunge the useless items from the PDB file (27). Following this, the structure was checked for any missing residues using the free Maestro 11.2 (5). Coordinates of 2'-deoxyuridine 5'-monophosphate (dUMP) and 5-fluoro-2'-deoxyuridine-5'-monophosphate (FdUMP) were retrieved from ChemSpider with ChemSpider ID: 58574 and 26330107 respectively (http://www.chemspider.com/Chemical-Structure.1906.html). Structures of other ligands were drawn in ChemSketch and were exported in the desired format for future use.

A web server namely CB-Dock was used for performing molecular docking. CB-Dock first identifies the putative binding sites automatically and then performs cavity sorting (38). According to the ligand to be docked it customizes the size of the docking (grid) box and finally performs molecular docking using AutoDock Vina (flexible docking tool) (6). The ligand poses are re-ranked as per docking score and the best binding pose is ascribed to the first confirmation. We used the knowledge from biology to select the most appropriate conformation. Further, before performing molecular docking we validated CB-Dock for its ability to detect active sites correctly through the self-docking protocol. Once it was assured that CB-Dock can reproduce the experimental binding site of the ligand we did our docking experiments using this web-based tool only. During docking of newly synthesized molecules against the 2'-deoxyuridine-5'-monophosphate (dUMP) binding site of thymidylate synthase, FdUMP was used as control. Ligands interact with protein receptors through various interactions comprising hydrophobic interactions, hydrogen bonds, salt bridges, and so on. For generating the interaction profile of biologically meaningful poses of various ligands individually in the docked state with thymidylate synthase, the respective files were prepared according to the desired format. A protein-ligand interaction profiler (PLIP) was used for exploring ligand-thymidylate synthase interactions. This web service has the potential to detect seven types of interactions existing between the ligand and receptor in docked state. These interactions encompass hydrophobic contacts, hydrogen bonds, pi-cation interactions, halogen bonds, salt bridges, pi-stacking, and water bridges.

4.2.2. *Gene expression analysis of Thymidylate Synthase in breast cancer.*

The Gepia2 database (http://gepia2.cancer-pku.cn/) is a web-based online data mining platform for exploring the gene expression data of normal samples and tumors (39). The database has 1085 breast tumor samples and 291 GTEx samples. The GEPIA2 was used to study the expression of TYMS in breast

tumor tissues. The UALCAN database (4), a comprehensive web resource for analyzing cancer OMICS data was further used to analyze the expression of TYMS in BC subclasses, age groups and ethnicities.

4.2.3 *Kaplan Meier Analysis.*

The Kaplan-Meier plotter (https://kmplot.com/), is a web resource with gene expression data and information regarding the survival of BC patients (10). The mRNA gene chip BC dataset of the KM Plotter has RFS data for 4929 and OS data for 1879 patients. The patients were grouped into two cohorts based on the median expression of the gene. The effect of the TYMS on OS and RFS of the two defined groups was analyzed by KM- survival curves and the hazard ratio intervals and log-rank P-value was calculated using the KM plotter.

4.3 Cell Culture

MCF-7, MDA-MB-231, and MDA-MB-468 human breast cancer cell lines were obtained from the National Centre for Cell Science (NCCS) in Pune. Prof Annapoorni Rangarajan, IISC, Bangalore, kindly supplied the murine cell line 4T1. Cell morphology was used to confirm the identification of these cells regularly. Dulbecco's Modified Eagle's Medium (DMEM; Thermo Fisher Scientific, Waltham, MA, United States) was used to culture MCF-7, MDA-MB-231, and MDA-MB-468 cells. 4T1 cells were cultured in RPMI1640 (Thermo Fisher Scientific, Waltham, MA, United States). The media was supplemented with 10% fetal bovine serum (FBS; Thermo Fisher Scientific, Waltham, MA, United States) and 1% penicillin-streptomycin (Thermo Fisher Scientific, Waltham, MA, United States). The cells were cultured in a CO2 incubator (5%) at 37°C.

4.3.1. *Cell Viability Assay*

MCF-7, MDA-MB-231, MDA-MB-468, and murine 4T1 human breast cancer cell lines were seeded in 96-well plates at $3x10^3$ cells/well. Following seeding, the cells were treated with uracil derivatives, which demonstrated substantial anticancer activity in early testing. The cells were treated with uracil derivatives in a dose - and time-dependent manner. The medium was replaced with MTT solution after 72 h of incubation, and the absorption of each well was then assessed at 490 nm. The inhibition of the production of formazan crystals was used as a cytotoxicity activity indicator. Non-linear regression analysis with Graph Pad software (v8) was performed to estimate the IC_{50} values on the cancer cells.

4.3.2. *Colony Formation Assay*

Cells were seeded onto six-well plates at a density of 1,000 cells per well and left to adhere for 24 hours. Cells were subsequently treated for 12 to 15 days with a continuous dosage of medicines in DMSO (final concentration 1%). The media was replaced after every 3 days and the wells were observed for colonies using an inverted microscope. After the colonies had grown large enough, the cells were fixed using 3.7 percent paraformaldehyde (in PBS). After that, cells were stained with a 0.05 percent crystal violet solution and photographed and analyzed with ImageJ software. For each cell type and therapeutic concentration, the experiment was carried out in biological triplicates.

Declarations

Funding: The work was supported by Research Grant sanctioned to Manzoor Ahmad Mir by Jammu Kashmir Science Technology and Innovation Council (JKST&IC), Department of Science and Technology, Govt of J&K vide Grant NO. JKST&IC/SRE/885-87 and Ramalinga Swami Fellowship, Grant No. BT/HRD/35/02/2006, sanctioned to Nissar Ahmad Wani from the Department of Biotechnology (DBT), Ministry of Science & Technology, New Delhi.

Acknowledgments: Umar Mehraj is a recipient of a junior research fellowship (JRF) from UGC-CSIR, Govt. of India. Nissar Ahmad Wani is the recipient of the Ramanujan Fellowship from the Science & Engineering Research Board (SERB), Department of Science and Technology, Govt. of India, New Delhi.

Conflict of Interest: All the authors declare that they have no known competing financial interests or personal relationships that could have appeared to influence the work reported in this paper.

Author contributions: Conceived and designed the experiments: MAM, MAZ, & NAW. In silico analysis: SAG, MAM & UM. Performed the experiments: MNL, & UM. Analyzed the data: MNL, MAM, SG, &, UM. Wrote the manuscript. MNL, MAM & UM. Revived and edited the manuscript NAW, SS, MAZ & MAM.

References

1. Bergstrom, D. E. (1982) Organometallic intermediates in the synthesis of nucleoside analogs. Nucleosides Nucleotides, **1**, 1–34.
2. Berman, H., Henrick, K. and Nakamura, H. (2003) Announcing the worldwide protein data bank. Nat. Struct. Mol. Biol., **10**, 980–980.
3. Brown, D. J. (2009) The pyrimidines. ed. John Wiley & Sons.
4. Chandrashekar, D. S., Bashel, B., Balasubramanya, S. A. H., Creighton, C. J., Ponce-Rodriguez, I., Chakravarthi, B. V. S. K. and Varambally, S. (2017) UALCAN: a portal for facilitating tumor subgroup gene expression and survival analyses. Neoplasia, **19**, 649–658.
5. Duan, J., Dixon, S. L., Lowrie, J. F. and Sherman, W. (2010) Analysis and comparison of 2D fingerprints: insights into database screening performance using eight fingerprint methods. J. Mol. Graph. Model., **29**, 157–170.
6. Eberhardt, J., Santos-Martins, D., Tillack, A. and Forli, S. (2021) AutoDock Vina 1.2. 0: new docking methods, expanded force field, and Python bindings.
7. Feng, J., Zhang, Z., Wallace, M. B., Stafford, J. A., Kaldor, S. W., Kassel, D. B., Navre, M., Shi, L., Skene, R. J. and Asakawa, T. (2007) Discovery of alogliptin: a potent, selective, bioavailable, and efficacious inhibitor of dipeptidyl peptidase IV. J. Med. Chem., **50**, 2297–2300.
8. Hayashi, Y. (2016) Pot economy and one-pot synthesis. Chemical science, **7**, 866–880.
9. Huang, M. and Graves, L. M. (2003) De novo synthesis of pyrimidine nucleotides; emerging interfaces with signal transduction pathways. Cellular and Molecular Life Sciences CMLS, **60**, 321–

336.

10. Lánczky, A. and Győrffy, B. (2021) Web-based survival analysis tool tailored for medical research (KMplot): development and implementation. J. Med. Internet Res., **23**, e27633.
11. Lebert, J. M., Lester, R., Powell, E., Seal, M. and McCarthy, J. (2018) Advances in the systemic treatment of triple-negative breast cancer. Current oncology, **25**, 142–150.
12. Lipinski, C. A., Lombardo, F., Dominy, B. W. and Feeney, P. J. (1997) Experimental and computational approaches to estimate solubility and permeability in drug discovery and development settings. Advanced drug delivery reviews, **23**, 3–25.
13. Longley, D. B., Harkin, D. P. and Johnston, P. G. (2003) 5-fluorouracil: mechanisms of action and clinical strategies. Nature reviews cancer, **3**, 330–338.
14. Lu, G.-q., Li, X.-y., Wang, D. and Meng, F.-h. (2019) Design, synthesis and biological evaluation of novel uracil derivatives bearing 1, 2, 3-triazole moiety as thymidylate synthase (TS) inhibitors and as potential antitumor drugs. Eur. J. Med. Chem., **171**, 282–296.
15. Ma, H., Jiang, W.-R., Robledo, N., Leveque, V., Ali, S., Lara-Jaime, T., Masjedizadeh, M., Smith, D. B., Cammack, N. and Klumpp, K. (2007) Characterization of the metabolic activation of hepatitis C virus nucleoside inhibitor β-d-2'-deoxy-2'-fluoro-2'-C-methylcytidine (PSI-6130) and identification of a novel active 5'-triphosphate species. J. Biol. Chem., **282**, 29812–29820.
16. McKeage, K. (2015) Trelagliptin: first global approval. Drugs, **75**, 1161–1164.
17. Mehraj, U., Aisha, S., Sofi, S. and Mir, M. A. (2022) Expression pattern and prognostic significance of baculoviral inhibitor of apoptosis repeat-containing 5 (BIRC5) in breast cancer: A comprehensive analysis. Advances in Cancer Biology-Metastasis, 100037.
18. Mehraj, U., Dar, A. H., Wani, N. A. and Mir, M. A. (2021) Tumor microenvironment promotes breast cancer chemoresistance. Cancer chemotherapy and pharmacology, 1–12.
19. Mehraj, U., Ganai, R. A., Macha, M. A., Hamid, A., Zargar, M. A., Bhat, A. A., Nasser, M. W., Haris, M., Batra, S. K. and Alshehri, B. (2021) The tumor microenvironment as driver of stemness and therapeutic resistance in breast cancer: New challenges and therapeutic opportunities. Cell. Oncol., 1–21.
20. Mehraj, U., Qayoom, H. and Mir, M. A. (2021) Prognostic significance and targeting tumor-associated macrophages in cancer: new insights and future perspectives. Breast Cancer, 1–17.
21. Mehraj, U., Wani, N. A., Hamid, A., Alkhanani, M., Almilaibary, A. and Mir, M. A. (2022) Adapalene inhibits the growth of triple-negative breast cancer cells by S-phase arrest and potentiates the antitumor efficacy of GDC-0941. Frontiers in Pharmacology, **13**, 958443.
22. Mir, M. A., Qayoom, H., Mehraj, U., Nisar, S., Bhat, B. and Wani, N. A. (2020) Targeting different pathways using novel combination therapy in triple negative breast Cancer. Curr. Cancer Drug Targets, **20**, 586–602.
23. Pałasz, A. and Cież, D. (2015) In search of uracil derivatives as bioactive agents. Uracils and fused uracils: Synthesis, biological activity and applications. Eur. J. Med. Chem., **97**, 582–611.

24. Paschall, A. V., Yang, D., Lu, C., Choi, J.-H., Li, X., Liu, F., Figueroa, M., Oberlies, N. H., Pearce, C. and Bollag, W. B. (2015) H3K9 trimethylation silences Fas expression to confer colon carcinoma immune escape and 5-fluorouracil chemoresistance. The Journal of Immunology, **195**, 1868–1882.
25. Pasha, N. and Turner, N. C. (2021) Understanding and overcoming tumor heterogeneity in metastatic breast cancer treatment. Nature Cancer, 1–13.
26. Pereira, M. A., Ramos, M. F. K. P., Dias, A. R., Faraj, S. F., dos Santos Cirqueira, C., de Mello, E. S., Zilberstein, B., Alves, V. A. F. and Ribeiro Jr, U. (2018) Immunohistochemical expression of thymidylate synthase and prognosis in gastric cancer patients submitted to fluoropyrimidine-based chemotherapy. Chinese Journal of Cancer Research, **30**, 526.
27. Pettersen, E. F., Goddard, T. D., Huang, C. C., Couch, G. S., Greenblatt, D. M., Meng, E. C. and Ferrin, T. E. (2004) UCSF Chimera—a visualization system for exploratory research and analysis. J. Comput. Chem., **25**, 1605–1612.
28. Qayoom, H., Wani, N. A., Alshehri, B. and Mir, M. A. (2021) An insight into the cancer stem cell survival pathways involved in chemoresistance in triple-negative breast cancer. Future Oncol.
29. Ramesh, D., Vijayakumar, B. G. and Kannan, T. (2020) Therapeutic potential of uracil and its derivatives in countering pathogenic and physiological disorders. Eur. J. Med. Chem., 112801.
30. Rose, M. G., Farrell, M. P. and Schmitz, J. C. (2002) Thymidylate synthase: a critical target for cancer chemotherapy. Clin. Colorectal Cancer, **1**, 220–229.
31. Shah, A., Nosheen, E., Zafar, F., Dionysiou, D. D., Badshah, A. and Khan, G. S. (2012) Photochemistry and electrochemistry of anticancer uracils. Journal of Photochemistry and Photobiology B: Biology, **117**, 269–277.
32. Shi, H., Han, Z., Liu, J., Xue, J., Zhang, S., Zhu, Z., Xia, J. and Huang, M. (2017) Comparing efficacy of lamivudine, adefovir dipivoxil, telbivudine, and entecavir in treating nucleoside analogues naive for HBeAg-negative hepatitis B with medium hepatitis B virus (HBV) DNA levels. Medical science monitor: international medical journal of experimental and clinical research, **23**, 5230.
33. Singh, A., Biot, C., Viljoen, A., Dupont, C., Kremer, L., Kumar, K. and Kumar, V. (2017) 1H-1, 2, 3-triazole-tethered uracil-ferrocene and uracil-ferrocenylchalcone conjugates: Synthesis and antitubercular evaluation. Chem. Biol. Drug Des., **89**, 856–861.
34. Sofi, S., Mehraj, U., Qayoom, H., Aisha, S., Almilaibary, A., Alkhanani, M. and Mir, M. A. (2022) Targeting cyclin-dependent kinase 1 (CDK1) in cancer: molecular docking and dynamic simulations of potential CDK1 inhibitors. Medical Oncology, **39**, 1–15.
35. Sofi, S., Mehraj, U., Qayoom, H., Aisha, S., Asdaq, S. M. B., Almilaibary, A. and Mir, M. A. (2022) Cyclin-dependent kinases in breast cancer: expression pattern and therapeutic implications. Medical Oncology, **39**, 1–16.
36. Sung, H., Ferlay, J., Siegel, R. L., Laversanne, M., Soerjomataram, I., Jemal, A. and Bray, F. (2021) Global cancer statistics 2020: GLOBOCAN estimates of incidence and mortality worldwide for 36 cancers in 185 countries. CA Cancer J. Clin., **71**, 209–249.

37. Takemura, Y. and Jackman, A. L. (1997) Folate-based thymidylate synthase inhibitors in cancer chemotherapy. Anticancer Drugs, **8**, 3–16.
38. Tan, H.-X., Gong, W.-Z., Zhou, K., Xiao, Z.-G., Hou, F.-T., Huang, T., Zhang, L., Dong, H.-Y., Zhang, W.-L. and Liu, Y. (2020) CXCR4/TGF-β1 mediated hepatic stellate cells differentiation into carcinoma-associated fibroblasts and promoted liver metastasis of colon cancer. Cancer Biology & Therapy, **21**, 258–268.
39. Tang, Z., Li, C., Kang, B., Gao, G., Li, C. and Zhang, Z. (2017) GEPIA: a web server for cancer and normal gene expression profiling and interactive analyses. Nucleic Acids Res., **45**, W98-W102.
40. Thomson, J. M. and Lamont, I. L. (2019) Nucleoside analogues as antibacterial agents. Front. Microbiol., **10**, 952.
41. Veber, D. F., Johnson, S. R., Cheng, H.-Y., Smith, B. R., Ward, K. W. and Kopple, K. D. (2002) Molecular properties that influence the oral bioavailability of drug candidates. J. Med. Chem., **45**, 2615–2623.
42. Wahba, H. A. and El-Hadaad, H. A. (2015) Current approaches in treatment of triple-negative breast cancer. Cancer biology & medicine, **12**, 106.
43. Wu, C.-H., Wu, C.-C. and Ho, Y.-S. (2007) Antitumor activity of combination treatment of Lentinus edodes mycelium extracts with 5-fluorouracil against human colon cancer cells xenografted in nude mice. J Cancer Mol, **3**, 15–22.
44. Xie, P., Mo, J.-L., Liu, J.-H., Li, X., Tan, L.-M., Zhang, W., Zhou, H.-H. and Liu, Z.-Q. (2020) Pharmacogenomics of 5-fluorouracil in colorectal cancer: review and update. Cell. Oncol., **43**, 989–1001.
45. Zhang, W., Feng, M., Zheng, G., Chen, Y., Wang, X., Pen, B., Yin, J., Yu, Y. and He, Z. (2012) Chemoresistance to 5-fluorouracil induces epithelial–mesenchymal transition via up-regulation of Snail in MCF7 human breast cancer cells. Biochem. Biophys. Res. Commun., **417**, 679–685.

Figures

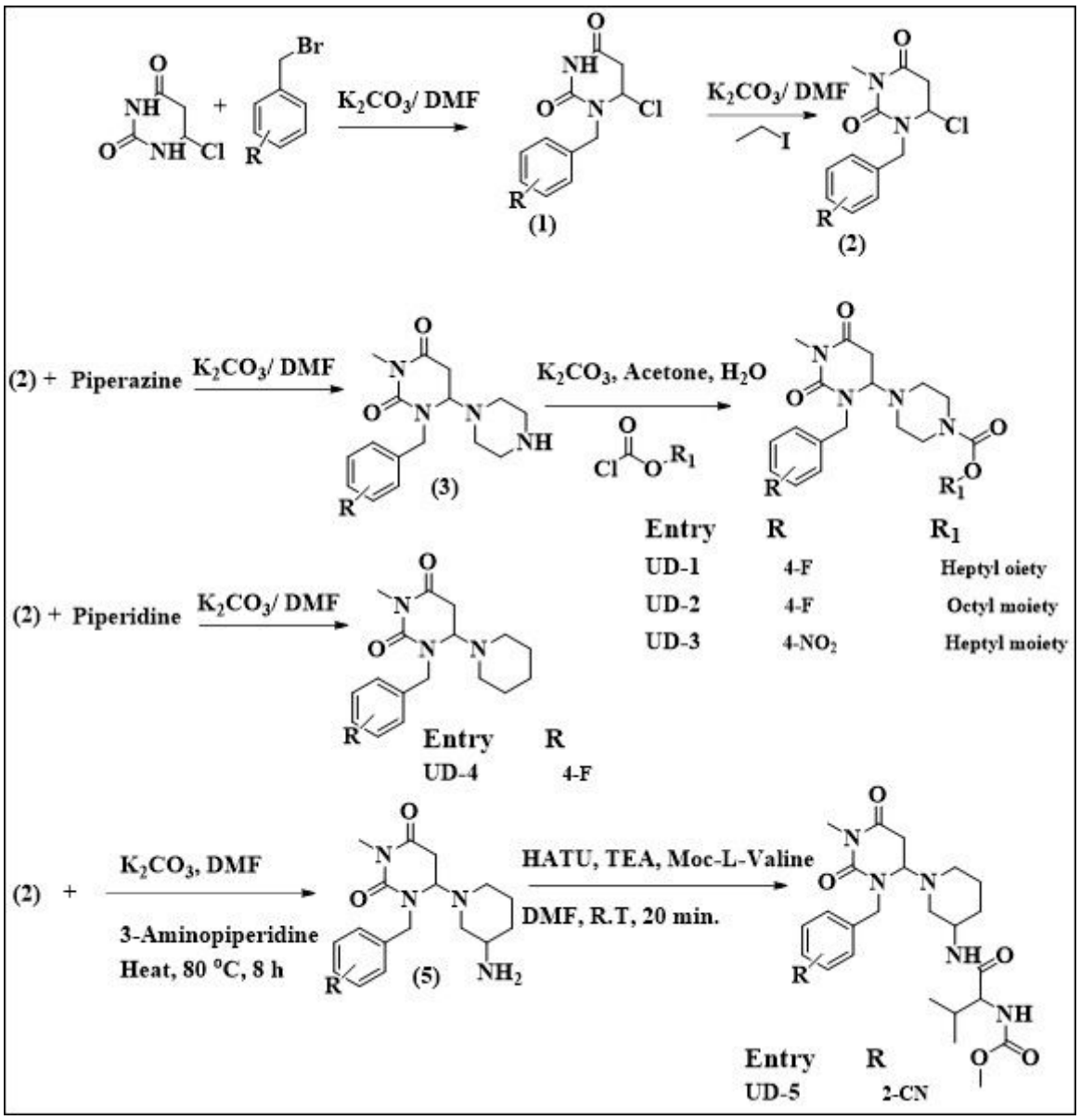

Figure 1

Schematic for the synthesis of novel uracil derivatives.

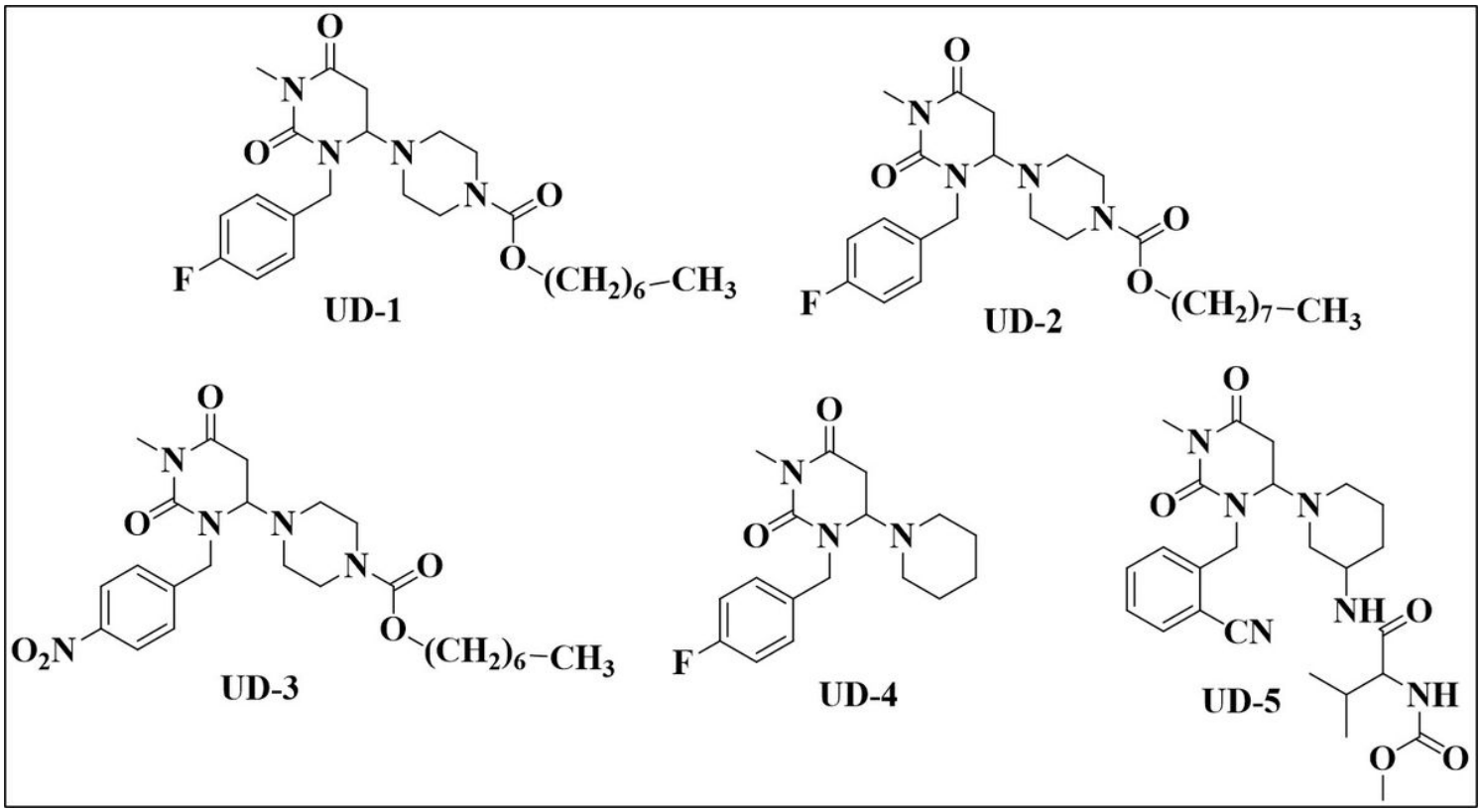

Figure 2

The chemical structures of synthesized uracil derivatives.

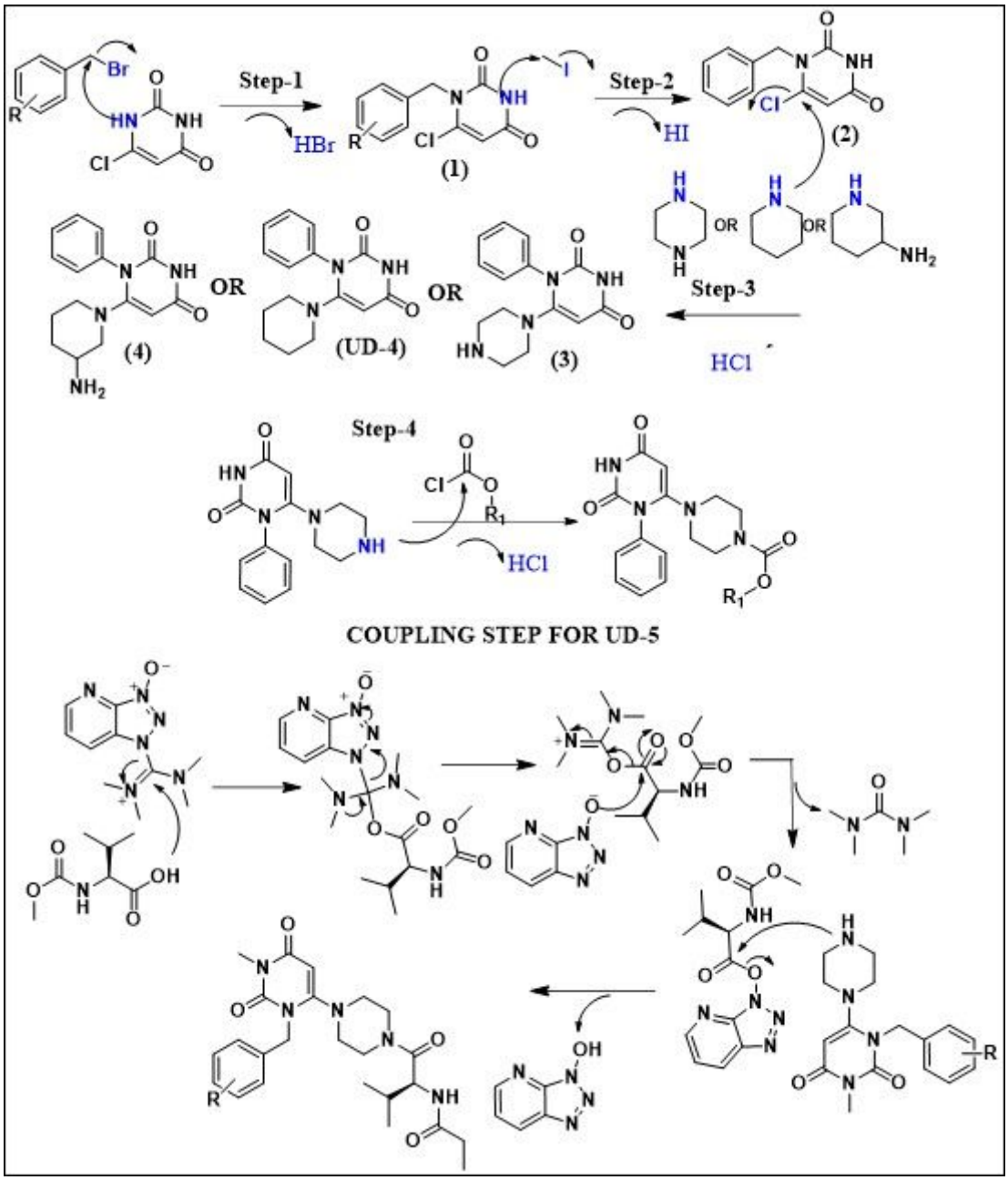

Figure 3

Scheme for the proposed mechanism for the synthesis of uracil derivatives.

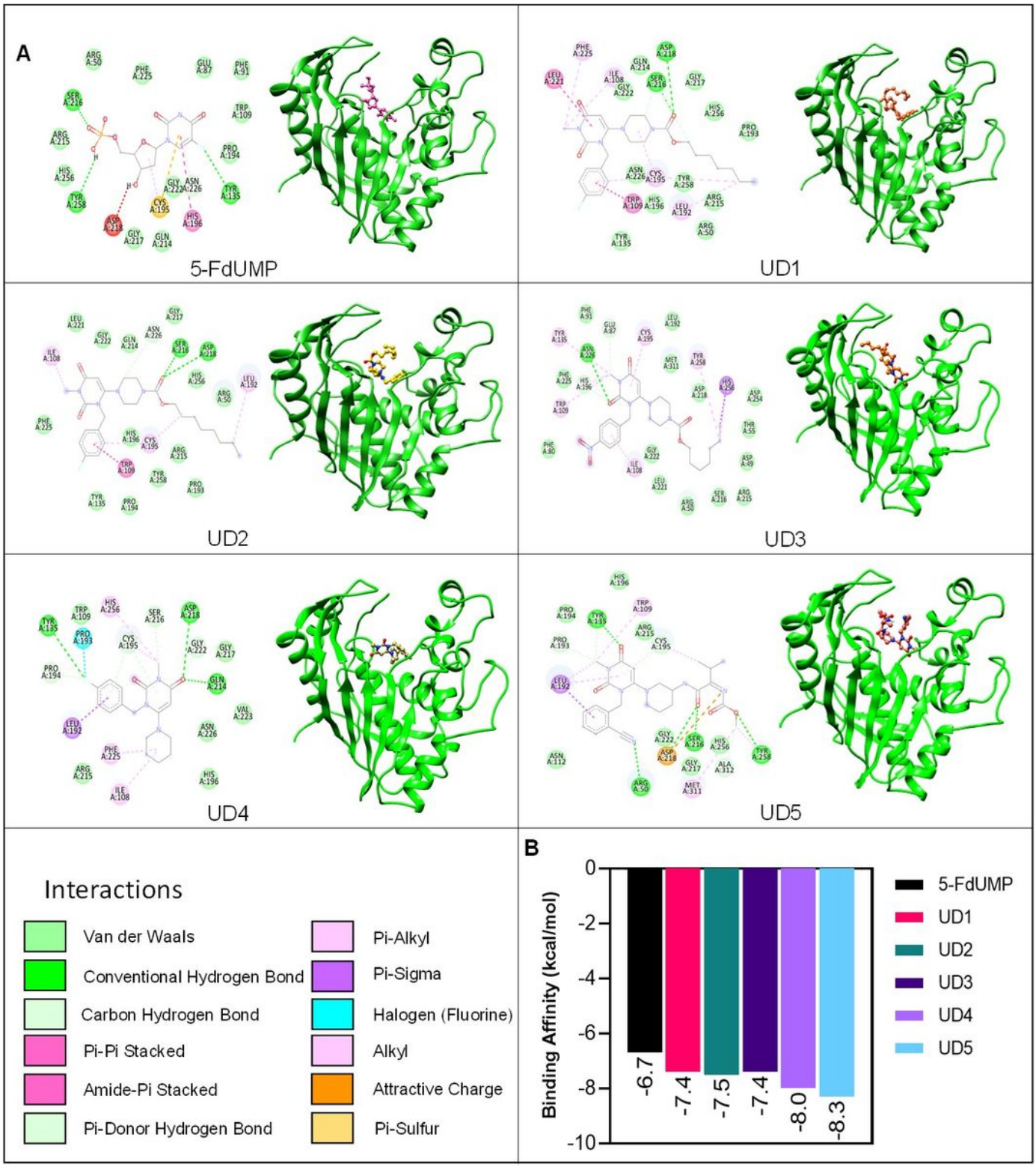

Figure 4

In silico evaluation of the binding affinity of novel UDs with thymidylate synthase, A. CB-Dock server can predict active site correctly. The green region shows the thymidylate synthase enzyme and the yellow-colored molecule (ball and stick) indicates its co-crystallized ligand. We separated this co-crystallized ligand from thymidylate synthase and then redocked it with this synthase using the CB-Dock server. The redocked ligand (red-colored) and co-crystallized ligand (yellow) colocalized at the same place. This

shows that the docking algorithm can predict the binding site correctly. We also analyzed the interaction profile of UDs with thymidylate synthase in 2D view. While 6 interactions were observed both in the case of UD4 and UD6. Relatively more interactions were observed with UD4 and UD5 in contrast to other UDs. **B.** Binding affinity values of newly synthesized five molecules against human thymidylate synthase. 5-FdUMP (FdUMP) (5-FU metabolite), the known binder of thymidylate synthase was put as control. The more negative value of binding affinity signifies stronger binding. Among the tested molecules, UD5 followed by UD4 and UD2 proved to be strong binders of thymidylate synthase as indicated by the binding affinity values. Further, all the novel molecules proved to be relatively more effective binders than the known metabolite of 5FU namely FdUMP.

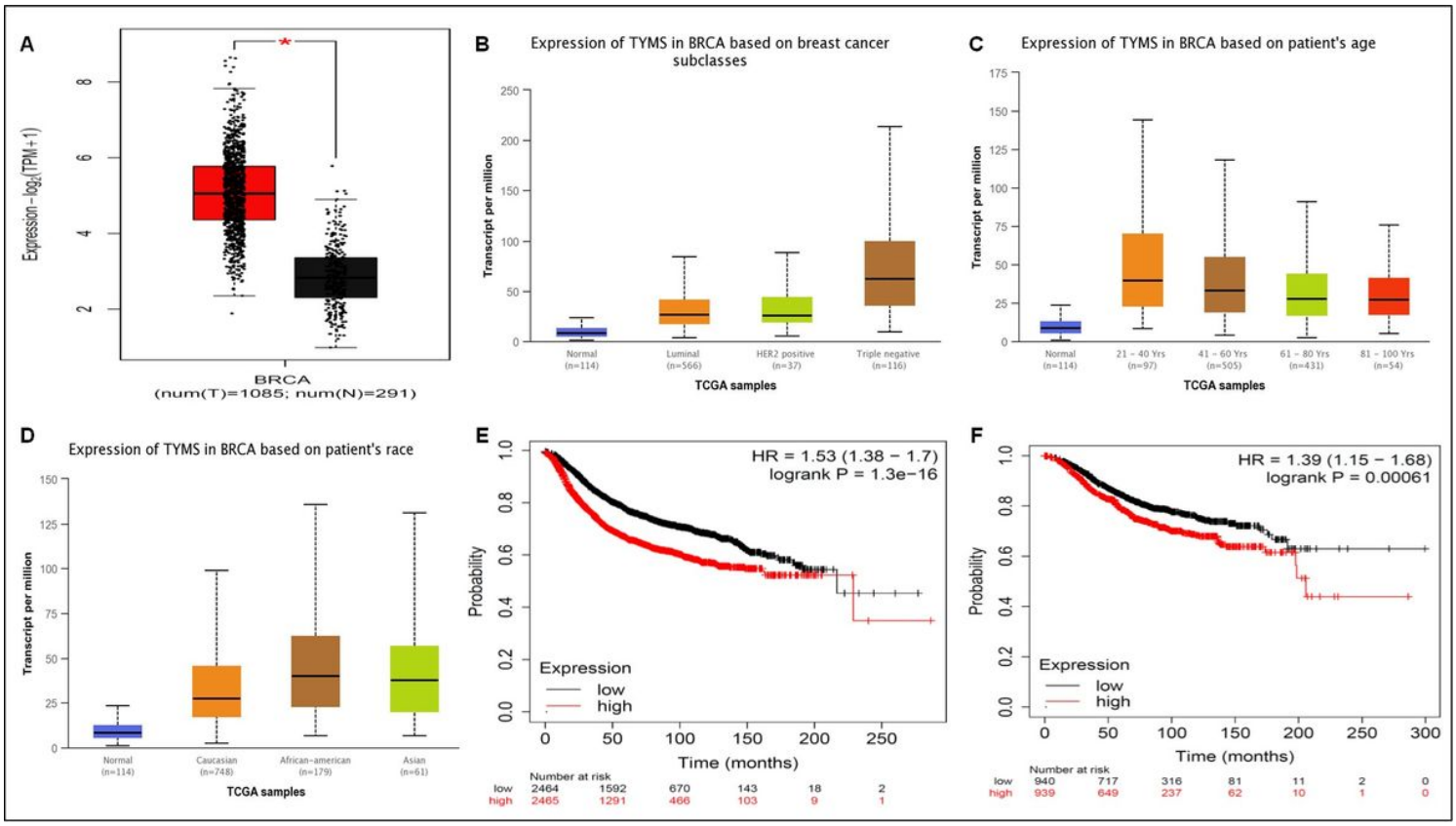

Figure 5

Expression pattern and prognostic significance of thymidylate synthase (TYMS) in breast cancer. A. TYMS was found high upregulated in BC patients compared to normal control or solid normal samples. **B.** Among breast cancer subtypes, TYMS showed high expression in aggressive subtypes viz TNBC followed by luminal and HER2 enriched. **C.** Enhanced expression of TYMS was observed among women under the age group of 21-40 yrs and, **D.**African-American women. **E.** High expression of TYMS was found associated with worse relapse-free survival (RFS) and **F.** overall survival (OS).

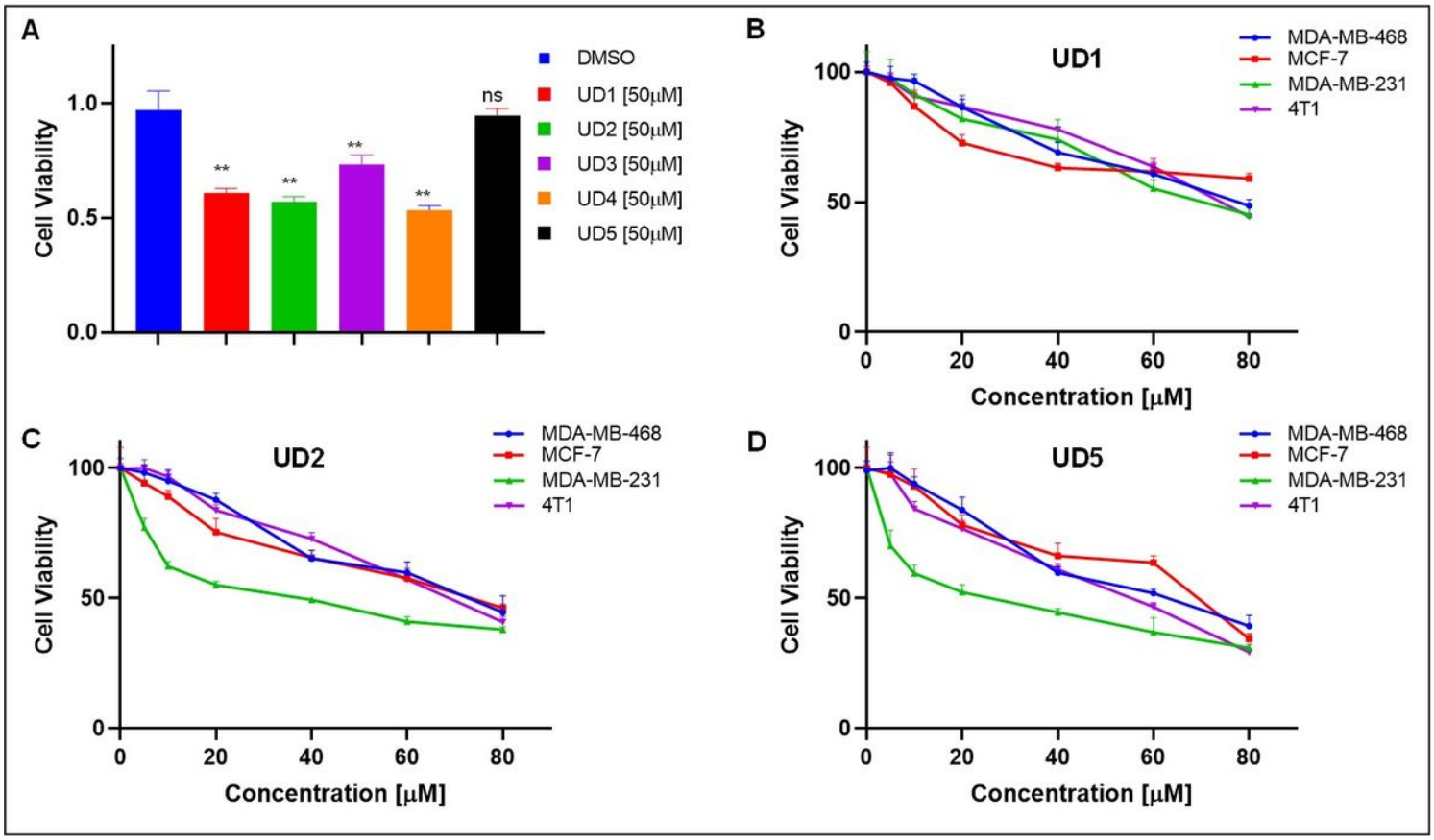

Figure 6

Uracil derivatives reduce the cell viability of breast cancer cell lines in a dose-dependent manner. A. Reduced cell viability of MDA-MB-231 cells treated with 50 μM of UDs for 72 hrs. Among the screened UDs, UD1, UD2 and UD4 showed high potency in reducing cell viability at 50 μM conc. One-way Annova was used for statistical analysis. $p < 0.0001$ (**, significantly different from DMSO treated controls. **B,** UD1, **C,** UD2, and **D.** UD4 were analyzed for potency in a panel of BC cell lines and showed an enhanced reduction in cell viability in a dose-dependent manner. The IC50 values were calculated using non-linear regression (curve fit) in Graphpad Prism V8. Among the three potent UDs, UD4 showed the highest reduction in cell viability and lowest IC50 value.

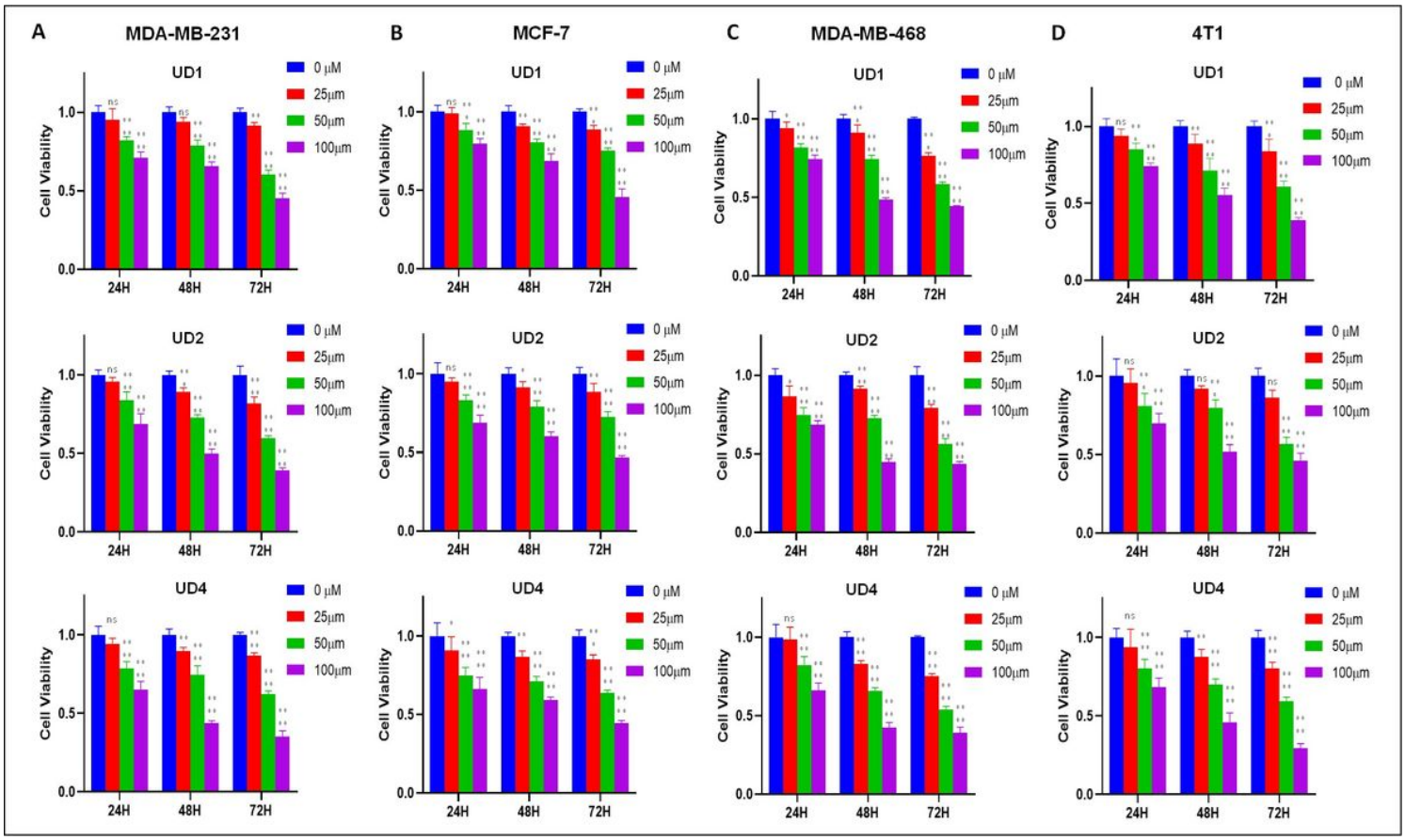

Figure 7

Uracil derivatives reduced the proliferation of breast cancer cell lines in a time-dependent manner. We next evaluated the effect of potent UDs, viz UD1, UD2, and UD2 on BC cell lines in a time-dependent manner, and the statistical significance increased with time. **A.** MDA-MB-231 cells, **B.** MCF-7 cells, **C.** MDA-MB-468 cells, and **D.** 4T1 cells demonstrated a reduction in cell viability with time upon treatment with UDs. Two-way annova was used for statistical analysis followed by Dunnett's multiple comparisons test. $p > 0.01$ (ns), $p < 0.01$ (*), $p < 0.001$ (**), $p < 0.005$ (***), $p < 0.0001$ (****).

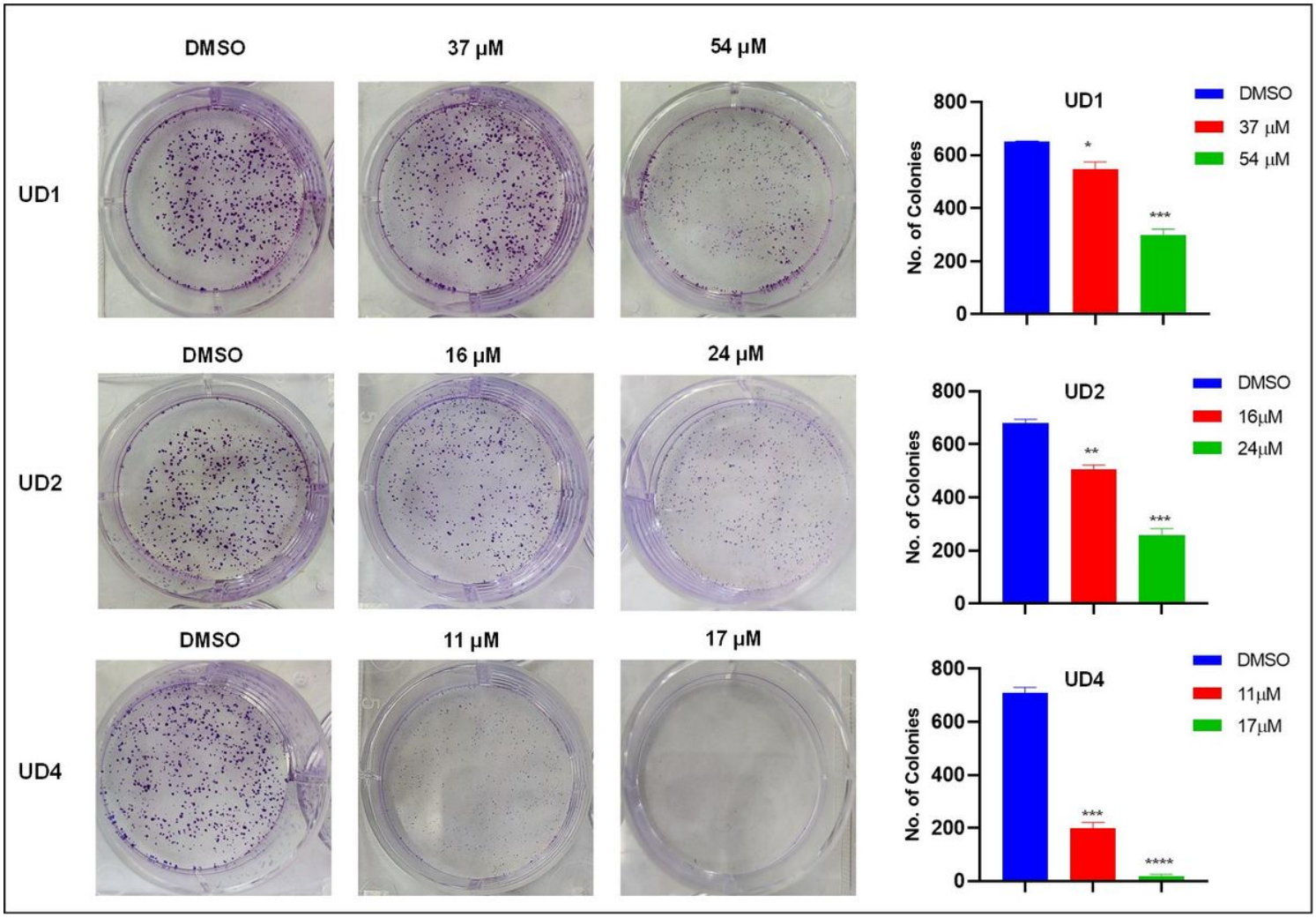

Figure 8

Uracil derivatives reduced colony formation potential of MDA-MB-231 cells. The effect of UDs on colony formation was evaluated and a significant reduction in colony formation was observed at conc lower than IC50 values. Among UDs, UD4 showed an enhanced reduction in cell colonies at 17 µM conc. One-way annova was used for statistical analysis followed by Dunnett's multiple comparisons test. $p < 0.01$ (*), $p < 0.001$ (**), $p < 0.005$ (***), $p < 0.0001$ (****).

Supplementary Files

This is a list of supplementary files associated with this preprint. Click to download.

- GraphicalAbstract.jpg
- SupplementaryData.pdf
- CompoundCharacterizationChecklist.pdf